ELSEVIER

Robotics and Autonomous Systems 21 (1997) 249–261

Robotics and Autonomous Systems

Robot planning and control

Oussama Khatib *, Sean Quinlan, David Williams

Robotics Laboratory, Department of Computer Science, Stanford University, Stanford, CA 94305, USA

Abstract

Planning and control are two basic components of autonomous robot systems. In recent years, significant advances have been made in both these areas. However, these developments have continued to be carried out in isolation, and the gap between planning and control remains an important one. This article discusses the ongoing effort at Stanford University for the extension of real-time robot control capabilities in the context of integrated robot planning and control. The goal is to develop a layer of real-time sensor-based motion primitives that connects planning and control. The article presents the basic models and methodologies developed for addressing this research area.

Keywords: Task-oriented robot control; Fine motion strategies; Real-time motion planning; Integrated planning and control; Cooperative mobile manipulation

1. Introduction

The past decade has seen considerable progress in robot planning and control. Efficient planning algorithms have been developed and tested on what were previously considered very large and difficult motion planning problems [4]. Dynamic, robust, and adaptive control techniques have been designed and validated for various types of robot mechanisms. Planning and control, however, have continued to be treated as two separate problems: planning is expected to provide complete and precise motion descriptions, and control is supposed to carry out the execution of these well-determined motion tasks. This separation of planning and control is illustrated in the two-level architecture shown in Fig. 1. Since the role of real-time control, in this architecture, is limited to the execution of predefined elementary tasks, the robot's interaction with the environment only takes place at the planning level. Given the relatively slow time-cycle of planning algorithms, the result is a robot system with little reactivity and limited real-time capabilities.

The development of autonomous robot systems requires tight coupling of planning, sensing, and execution. These functions must operate together for effective behavior in a changing and uncertain environment. One aspect of this problem concerns the control architecture [2,6] needed for the integration of these functionalities. The second aspect concerns the framework within which this integration can be accomplished. The development of such a framework has been precisely one of the primary objectives of the effort reported in this article. The aim is to develop a general framework for task-oriented sensor-based robot control, with strong emphasis on the connections with both perception and planning.

The general architecture we are pursuing is illustrated in Fig. 2. In this architecture, the connection between planning and execution relies on the integration of a layer of real-time sensor-based action primitives.

* Corresponding author. E-mail: ok@flamingo.stanford.edu.

PII S0921-8890(96)00078-4

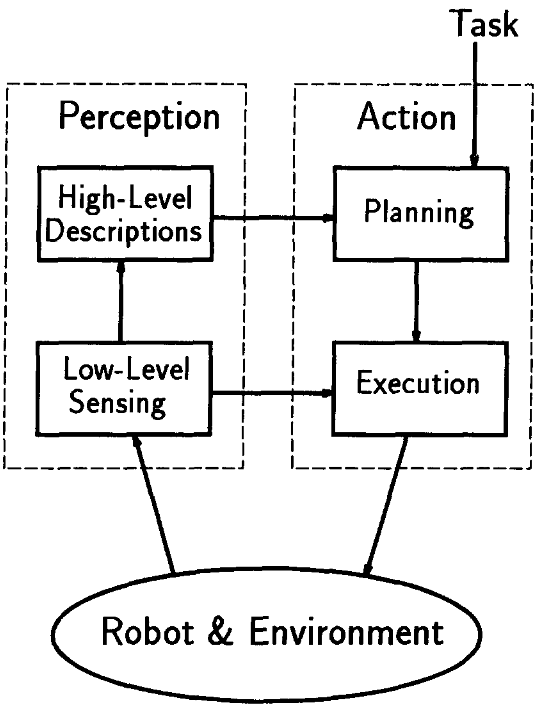

Fig. 1. Conventional architecture.

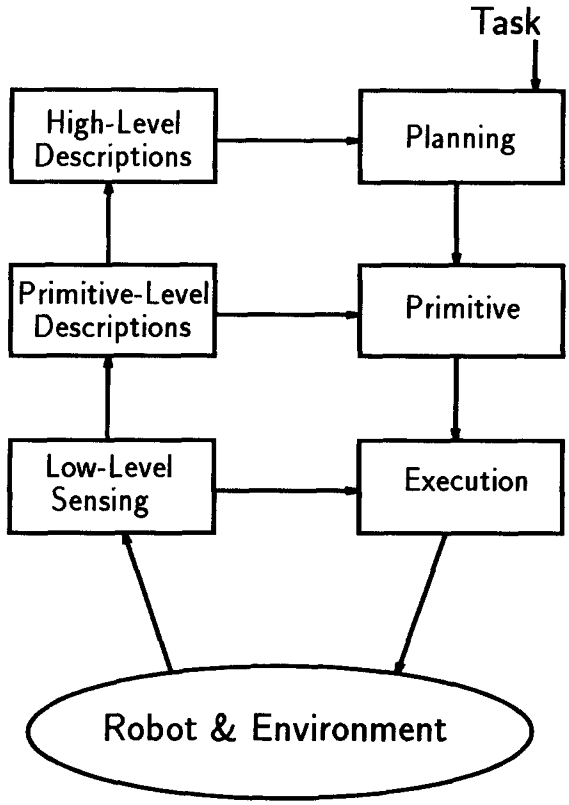

Fig. 2. Robotic system architecture.

For each action primitive, there is a matched set of sensing capabilities, ranging from low-level sensing to high-level perceptual descriptions. The entire system is a hierarchy of sensing-action loops, low-level sensing feeding low-level actions (at high rates) and high-level perceptual descriptions feeding planning (at low rates).

The construction of such a system relies on the design of control strategies that can deal with the robot's object-level behavior, and the development of general frameworks for the integration of these strategies with global planning systems. The article presents the basic models and methodologies developed to address these two research areas.

2. Object-level manipulation

Robot dynamics has been viewed traditionally from the perspective of a manipulator's joint motions, and significant effort has been devoted to the development of *joint space* dynamic models and control methodologies. However, the limitations of joint space control techniques, especially in constrained motion tasks, have motivated alternative approaches for dealing with task-level dynamics and control. The *operational space formulation*, which falls within this line of research, has been driven by the need to develop mathematical models for the description, analysis, and control of robot dynamics with respect to task behavior.

Below, we briefly discuss the various control methodologies that have been developed within this framework. These include: the *unified motion and force control* approach; the notion of *dynamic consistency* in redundant manipulator control; the *reduced effective inertia* property associated with macro-/mini-manipulator systems and the *dynamic coordination* strategy proposed for their control; and the *augmented-object* model for the control of robot systems involving multiple manipulators and the *virtual linkage* model for the description and control of object internal forces in multi-grasp manipulation. We also describe the extension of these models to mobile manipulator systems.

2.1. End-effector dynamics

The difficulty with joint space control techniques lies in the discrepancy between the space where robot tasks are specified and the space in which the control is taking place. By its very nature, joint space control calls for transformations whereby joint space descriptions are obtained from the robot task specifications. The task transformation problem associated with joint space control has been the basic motivation for much of the early work in task-level control schemes [10,18,22,31].

In manipulator control, higher velocities and accelerations result in higher dynamic interaction forces between the moving links. Active compensation for the effects of these forces is then required for achieving dynamic accuracy. Techniques for dynamic decoupling and motion control are well developed. These methodologies are generally based on the joint space equations of motion of the manipulator,

$$A(\boldsymbol{q})\ddot{\boldsymbol{q}} + \boldsymbol{b}(\boldsymbol{q}, \dot{\boldsymbol{q}}) + \boldsymbol{g}(\boldsymbol{q}) = \boldsymbol{\Gamma}; \tag{1}$$

where $\boldsymbol{q}$ is the n joint coordinates, $A(\boldsymbol{q})$ the $n \times n$ kinetic energy matrix, $\boldsymbol{b}(\boldsymbol{q}, \dot{\boldsymbol{q}})$ the vector of centrifugal and Coriolis joint-forces, $\boldsymbol{g}(\boldsymbol{q})$ the gravity joint-force vector and $\boldsymbol{\Gamma}$ is the vector of generalized joint-forces.

Beyond the costly transformations it requires, joint space control is incompatible with the requirements of constrained tasks that involve simultaneous motion and force control. Joint space dynamic models provide a description of the dynamic interaction between joint axes. However, what is needed in the analysis and design of force control algorithms is a description of the dynamic interaction between the end effector or manipulated object and mating parts. In the absence of such descriptions, most of the research in force control has been driven by kinematic and static considerations. Compliant motion control has been achieved through the use of inner loops of position or velocity control [29,35]. While position-based or velocity-based compliant motion control have been successfully used in many quasi-static operations, their performance in dynamic tasks has been very limited. The limitations of control gains associated with these techniques have generally resulted in slow and sluggish behavior. Hybrid position/force control [28] and non-dynamic implementations of impedance control have also resulted in limited dynamic performance.

The basic idea in the operational space approach [12,14] is to control motions and contact forces through the use of control forces that act directly at the level of the end effector. These control forces are produced by the application of corresponding torques and forces at the manipulator joints. High performance control of end-effector motions and contact forces requires the construction of a model describing the dynamic behavior as perceived at the end effector, or, more precisely, at the point on the effector where the task is specified. This point is called the *operational point*. The construction of the end-effector dynamic model is achieved by expressing the relationship between its positions, velocities and accelerations, and the operational forces acting on it. For a non-redundant manipulator, the operational space equations of motion of a manipulator are [14]

$$\Lambda(\boldsymbol{x})\ddot{\boldsymbol{x}} + \boldsymbol{\mu}(\boldsymbol{x}, \dot{\boldsymbol{x}}) + \boldsymbol{p}(\boldsymbol{x}) = \boldsymbol{F}, \tag{2}$$

where $\boldsymbol{x}$ is the vector of the m operational coordinates describing the position and orientation of the effector, $\Lambda(\mathbf{x})$ the $m \times m$ kinetic energy matrix associated with the operational space and $\boldsymbol{\mu}(\boldsymbol{x}, \dot{\boldsymbol{x}}), \boldsymbol{p}(\boldsymbol{x})$, and $\boldsymbol{F}$ are, respectively, the centrifugal and Coriolis force vector, gravity force vector, and generalized force vector acting in operational space,

The operational space model provides the foundation for a unified approach to task-level motion and force control. The operational forces are produced by submitting the manipulator to the corresponding joint forces, using a simple force transformation. The relationship between operational forces, $\boldsymbol{F}$, and joint forces, $\boldsymbol{\Gamma}$ is

$$\boldsymbol{\Gamma} = J^{\mathrm{T}}(\boldsymbol{q})\boldsymbol{F}; \tag{3}$$

where $J(\boldsymbol{q})$ is the Jacobian matrix.

The use of the forces generated at the end effector to control motions leads to a natural integration of active force control. In the operational space framework, simultaneous control of motions and forces is achieved by a unified command vector for controlling both the motions and forces at the operational point.

2.2. Unified motion/force control

By the nature of coordinates associated with spatial rotations, operational forces acting along rotation coordinates are not homogeneous to moments, and vary with the type of representation being used (e.g., Euler angles, direction cosines, Euler parameters, quaternions). Although this characteristic does not raise any difficulty in free motion operations, the homogeneity issue is important in tasks where both motions and active forces are involved. This issue is also a concern in the analysis of inertial properties. These properties are expected to be independent of the type of representation used for the description of the end-effector orientation.

The homogeneity issue is addressed by using the relationships between operational velocities and instantaneous angular velocities. The Jacobian matrix $J(\boldsymbol{q})$ associated with a given selection, $\mathbf{x}$, of operational coordinates can be expressed [14] as

$$J(\boldsymbol{q}) = E(\boldsymbol{x}) J_0(\boldsymbol{q}), \tag{4}$$

where the matrix $J_0(\boldsymbol{q})$, termed *the basic Jacobian*, is defined independently of the particular set of parameters used to describe the end-effector configuration, whereas the matrix $E(\boldsymbol{x})$ is dependent on those parameters. The basic Jacobian establishes the relationships between generalized joint velocities $\dot{\boldsymbol{q}}$ and end-effector linear and angular velocities $\boldsymbol{v}$ and ω:

$$\vartheta \triangleq \begin{bmatrix} \boldsymbol{v} \\ \omega \end{bmatrix} = J_0(\boldsymbol{q})\dot{\boldsymbol{q}}. \tag{5}$$

Like angular velocities, moments are defined as instantaneous quantities. A generalized operational force vector, $\boldsymbol{F}$, associated with a set of operational coordinates, $\boldsymbol{x}$, is related to forces and moments by

$$\boldsymbol{F}_0 \triangleq \begin{bmatrix} \mathcal{F} \\ \mathcal{M} \end{bmatrix} = E^{\mathrm{T}}(\boldsymbol{x})\, \boldsymbol{F}, \tag{6}$$

where $\mathcal{F}$ and $\mathcal{M}$ are the vectors of forces and moments.

Compliant motion and part mating operations involve motion control in some directions and force control in the other directions. Such tasks are described by the *generalized selection matrix* Ω and its complement $\overline{\Omega}$ associated with motion control and force control, respectively [14].

With respect to linear and angular motions, the end-effector/sensor equations of motion can be written as

$$\Lambda_0(\boldsymbol{x})\dot{\vartheta} + \mu_0(\boldsymbol{x}, \vartheta) + \boldsymbol{p}_0(\boldsymbol{x}) + \boldsymbol{F}_{\text{contact}} = \boldsymbol{F}_0. \tag{7}$$

The vector $\boldsymbol{F}_{\text{contact}}$ represents the contact forces acting at the end effector. The unified approach for end-effector dynamic decoupling, motion, and active force control is achieved by selecting the control structure

$$\boldsymbol{F}_0 = \boldsymbol{F}_{\text{motion}} + \boldsymbol{F}_{\text{active-force}}, \tag{8}$$

where

$$\boldsymbol{F}_{\text{motion}} = \widehat{\Lambda}_0(\boldsymbol{x})\Omega\boldsymbol{F}^{\star}_{\text{motion}} + \widehat{\mu}_0(\boldsymbol{x}, \vartheta) + \widehat{\boldsymbol{p}}_0(\boldsymbol{x}), \tag{9}$$

$$\boldsymbol{F}_{\text{active-force}} = \widehat{\Lambda}_0(\boldsymbol{x})\overline{\Omega}\boldsymbol{F}^{\star}_{\text{active-force}} + \boldsymbol{F}_{\text{sensor}}, \tag{10}$$

and where $\widehat{.}$ represents estimates of the model parameters.

The vectors $\boldsymbol{F}^{\star}_{\text{motion}}$ and $\boldsymbol{F}^{\star}_{\text{active-force}}$ represent the inputs to the decoupled system. With perfect estimates of the dynamic parameters and perfect sensing of contact forces (i.e., $\boldsymbol{F}_{\text{sensor}} = \boldsymbol{F}_{\text{contact}}$), the closed loop system is described by the following two decoupled sub-systems:

$$\Omega\dot{\vartheta} = \Omega\boldsymbol{F}^{\star}_{\text{motion}}, \tag{11}$$

$$\overline{\Omega}\dot{\vartheta} = \overline{\Omega}\boldsymbol{F}^{\star}_{\text{active-force}}. \tag{12}$$

2.3. Redundancy and singularities

The joint space task transformation problem is exacerbated for mechanisms with redundancy or at kinematic singularities. The typical approach involves the use of pseudo- or generalized inverses to solve an under-constrained or degenerate system of linear equations, while optimizing some given criterion [8,11,34]. Other inverses with improved performance also have been investigated, e.g., the singularity robust inverse [7,23].

The operational space control of redundant manipulators relies on two basic models: a *task-level dynamic model* obtained by projecting the manipulator dynamics into the operational space, and a *dynamically consistent force/torque relationship* that provides decoupled control of joint motions in the null space associated with the redundant mechanism. Using this relationship, the end effector can be independently controlled by operational forces, while internal motions can be controlled by joint torques that are guaranteed not to alter the end effector's dynamic behavior.

The relationship between joint torques and operational forces for redundant manipulator is [17]

$$\boldsymbol{\Gamma} = J^{\mathrm{T}}(\boldsymbol{q})\boldsymbol{F} + [I - J^{\mathrm{T}}(\boldsymbol{q})\bar{J}^{\mathrm{T}}(\boldsymbol{q})]\boldsymbol{\Gamma}_0 \tag{13}$$

with

$$\bar{J}(\boldsymbol{q}) = A^{-1}(\boldsymbol{q})J^{\mathrm{T}}(\boldsymbol{q})\Lambda(\boldsymbol{q}) \tag{14}$$

where $\bar{J}(\boldsymbol{q})$ is the *dynamically consistent generalized inverse* [17] and $\Lambda(\boldsymbol{q})$ is the pseudo-kinetic energy matrix

$$\Lambda^{-1}(\boldsymbol{q}) = J(\boldsymbol{q})A^{-1}(\boldsymbol{q})J^{\mathrm{T}}(\boldsymbol{q}). \tag{15}$$

This relationship provides a decomposition of joint forces into two dynamically decoupled control vectors: joint forces corresponding to forces acting at the end effector ($J^{\mathrm{T}}\boldsymbol{F}$); and joint forces that only affect internal motions, ($[I - J^{\mathrm{T}}(\boldsymbol{q})\bar{J}^{\mathrm{T}}(\boldsymbol{q})]\boldsymbol{\Gamma}_0$).

The dynamic behavior at the end effector for a redundant manipulator is obtained by the projection of the joint-space equations of motion (1), by the *dynamically consistent* generalized inverse $\bar{J}^{\mathrm{T}}(\boldsymbol{q})$,

$$\begin{aligned} &\bar{J}^{\mathrm{T}}(\boldsymbol{q})[A(\boldsymbol{q})\ddot{\boldsymbol{q}} + \boldsymbol{b}(\boldsymbol{q},\dot{\boldsymbol{q}}) + \boldsymbol{g}(\boldsymbol{q}) = \boldsymbol{\Gamma}] \\ &\quad\Longrightarrow \Lambda(\boldsymbol{q})\ddot{\boldsymbol{x}} + \boldsymbol{\mu}(\boldsymbol{q},\dot{\boldsymbol{q}}) + \boldsymbol{p}(\boldsymbol{q}) = \boldsymbol{F} \end{aligned} \tag{16}$$

The above property also applies to non-redundant manipulators, where the matrix $\bar{J}^{\mathrm{T}}(\boldsymbol{q})$ reduces to $J^{-\mathrm{T}}(\boldsymbol{q})$.

In addition to their impact on the control of redundant manipulators, these models have been the basis for the development of an effective strategy for dealing with kinematic singularities [5]. With this strategy, a manipulator at a singular configuration is treated as a redundant system in the subspace orthogonal to the singular direction.

2.4. *Macro-/mini-manipulators*

High-performance control of forces and motions requires a robot structure to have a high mechanical bandwidth. Incorporating lightweight links, i.e., a mini-manipulator, at the end of the arm can greatly improve this bandwidth and significantly increase the ability of the manipulator to perform fine motions.

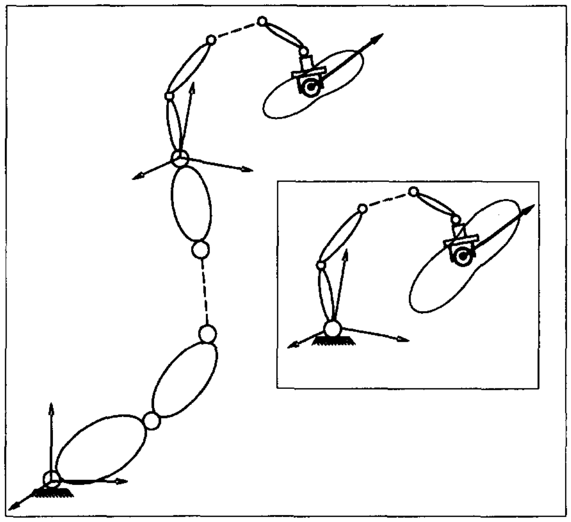

Fig. 3. Inertial properties of a macro-/mini-manipulator. The magnitudes of the inertial properties of the macro-/mini-manipulator system, at any configuration and in any direction, are smaller than or equal to the magnitudes of the inertial properties associated with the mini-manipulator. The inertial properties are visualized using the belted ellipsoid representation.

A macro-/mini-manipulator can be viewed as the mechanism resulting from the serial combination of two manipulators [16]. As illustrated in Fig. 3, the manipulator connected to the ground is the *macro-manipulator*, and the second manipulator, referred to as the *mini-manipulator*, is the structure formed by smallest distal set of degrees of freedom that span the operational space.

The magnitude of the inertial properties of macro-/mini-structure in a direction represented by a unit vector $\boldsymbol{w}$ in the m-dimensional space can be described by the scalar [17]

$$\sigma_{\mathrm{w}}(\Lambda) = \frac{1}{(\boldsymbol{w}^{\mathrm{T}}\Lambda^{-1}\boldsymbol{w})},$$

which represents the effective inertial properties in the direction $\boldsymbol{w}$.

Our analysis of macro-/mini-manipulator systems shows the inertial properties of these systems to possess an important characteristic: that of *reduced effective inertia*. We have found that, for all directions and configurations, the effective inertia of a macro-/mini-manipulator system is bounded above by the inertia of the mini-manipulator alone [17].

$$\sigma_{\mathrm{w}}(\Lambda) \leq \sigma_{\mathrm{w}}(\Lambda_{\mathrm{m}}), \tag{17}$$

where (Λ_{m}) is the kinetic energy matrix associated with the mini-manipulator [17].

High dynamic performance for the manipulated object task (motion and contact forces) can be achieved with the same operational space control structure used for non-redundant mechanisms. Minimizing the instantaneous kinetic energy, such a controller will attempt to carry out the entire task using essentially the fast dynamic response of the mini structure. However, given the mechanical limits on the mini structure's joint motions, this would rapidly lead to joint limitations of the mini-structure degrees of freedom.

To allow the mini-structure's high bandwidth to be fully utilized in wide range operations, we have proposed a *dynamic coordination strategy*, that uses the system's internal motions to minimize deviation from the midrange joint positions of the mini-manipulator. Effective implementation of this strategy relies on preventing any effects of the internal motion from influencing the primary end-effector task. This is achieved by implementing this strategy using the dynamically consistent relationship between joint torques and end-effector forces of Eq. (13).

2.5. *Multi-grasp manipulation*

Multi-arm control has also been treated as a motion coordination problem. One of the first schemes for the control of a two-arm system [3] was organized in a master/slave fashion, and used a motion coordination procedure to minimize errors in the relative position of the two manipulators. In another study [38], one manipulator was treated as a "leader" and the other as a "follower". Control of the follower was based on the constraint relationships between the two manipulators. In contrast, the two manipulators were given a symmetric role in the coordination proposed by Uchiyama and Dauchez [33]. The problem of controlling both motion and force in multi-arm systems has been investigated by Hayati [9]. In the proposed approach, the load is partitioned among the arms. Dynamic decoupling and motion control are then achieved at the level of individual manipulator effectors. In the force control subspace, the magnitude of forces is minimized. Tarn et al. [32] developed a closed chain dynamic model for a two-manipulator system with respect to a selected set of generalized joint coordinates. Non-linear feedback and output decoupling techniques were then used to linearize and control the system in task coordinates.

Analyzing the inertial properties of multi-arm robot systems, we have found an important additive property of parallel structures. It has been shown [15] that the inertial properties perceived at the manipulated object are given by the sum of the inertial properties associated with each individual manipulator and the inertial properties of the unconstrained object, all expressed with respect to the same operational point. Centrifugal, Coriolis, and gravity forces have also been shown to possess this additive property. Combining the dynamics of the individual manipulators and object, we have developed the *augmented object* model, which describes the dynamics at the operational point for the multi-arm robot system.

For a set of non-redundant manipulators, the *augmented object* model is

$$\Lambda_{\oplus}(\boldsymbol{x})\ddot{\boldsymbol{x}} + \boldsymbol{\mu}_{\oplus}(\boldsymbol{x}, \dot{\boldsymbol{x}}) + \boldsymbol{p}_{\oplus}(\boldsymbol{x}) = \boldsymbol{F}_{\oplus} \tag{18}$$

with

$$\Lambda_{\oplus}(\boldsymbol{x}) = \Lambda_{\mathcal{L}}(\boldsymbol{x}) + \sum_{i=1}^{N} \Lambda_i(\boldsymbol{x}), \tag{19}$$

where $\Lambda_{\mathcal{L}}(\boldsymbol{x})$ and $\Lambda_i(\boldsymbol{x})$ are the kinetic energy matrices associated with the object and the ith effector, respectively. The vectors $\boldsymbol{\mu}_{\oplus}(\boldsymbol{x}, \dot{\boldsymbol{x}}), \boldsymbol{p}_{\oplus}(\boldsymbol{x})$, and $\boldsymbol{F}_{\oplus}$ all have the additive property. This model has been extended to cooperative redundant manipulators [17].

In tasks involving large and heavy objects, a useful criterion for force distribution is minimization of total actuator activities [15]. In contrast, dextrous manipulation requires accurate control of internal forces. This problem has received wide attention and algorithms for internal force minimization [24] and grasp stability [21] have been developed. Addressing the problem of internal force in manipulation, we have proposed a physically based model, the *virtual linkage* [36], for the description and control of internal forces and moments in multi-grasp tasks.

In this model, grasp points are connected by a closed, non-intersecting set of virtual links. The

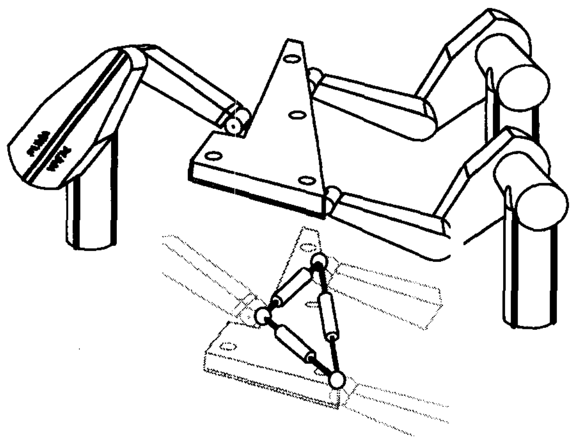

Fig. 4. The virtual linkage for three-grasp manipulation. The internal forces and moments on the manipulated object are represented by the 12-degree-of-freedom linkage formed by three spherical joints and three prismatic joints.

virtual linkage model is illustrated for an example of three-arm manipulation in Fig. 4. The kinematic structure of the virtual linkage for this manipulation task is one in which three actuated prismatic joints are connected by passive revolute joints to form a closed-chain, three-degree-of-freedom mechanism. A spherical joint with three actuators is then connected at each grasp point to resist internal moments.

The virtual linkage described above constitutes the basic structure for virtual linkages with additional grasps. Indeed, the virtual linkage model can be extended to any number of grasp points. Each additional grasp point results in six new actuator degrees of freedom which must be characterized by the virtual linkage.

Specifically, each new grasp introduces three internal forces and three internal moments. These are accounted for by introducing three more prismatic actuators and one more spherical joint to the linkage. This is accomplished by connecting new grasp points to existing grasp points through three actuated virtual members and one spherical joint.

In the case of an N-grasp manipulation task, a *virtual linkage* model is a $6(N-1)$-degree-of-freedom mechanism that has $3(N-2)$ linearly actuated members and N spherically actuated joints. Forces and moments applied at the grasp points of this linkage will cause forces and torques at its joints. We can independently specify internal forces in the $3(N-2)$ members, along with $3N$ internal moments at the spherical joints. Internal forces in the object are then characterized by these forces and torques in a physically meaningful way.

The relationship between applied forces, their resultant and internal forces is

$$\begin{bmatrix} \boldsymbol{F}_{\text{res}} \\ \boldsymbol{F}_{\text{int}} \end{bmatrix} = \boldsymbol{G} \begin{bmatrix} \boldsymbol{F}_1 \\ \vdots \\ \boldsymbol{F}_N \end{bmatrix}, \tag{20}$$

where $\boldsymbol{F}_{\text{res}}$ represents the resultant forces at the operational point, $\boldsymbol{F}_{\text{int}}$ the internal forces and $\boldsymbol{F}_i$ the forces applied at the grasp point i. $\boldsymbol{G}$ is called the grasp description matrix, and relates forces applied at each grasp to the resultant and internal forces in the object.

The augmented object and virtual linkage models have been successfully used in the manipulation of objects with three PUMA 560 manipulators [37].

2.6. Mobile manipulation

Mobile manipulation capability is key to many new applications of robotics in space, underwater, construction, and service environments. A central issue in the development of mobile manipulation systems is vehicle/arm coordination.

In our approach, a vehicle/arm system is viewed as the mechanism resulting from the serial combination of two sub-systems: a "macro" structure with coarse, slow, dynamic responses (the mobile base), and a relatively fast and accurate "mini" device (the manipulator). Treated as a macro/mini redundant mechanism, the vehicle/arm coordination is achieved using the same control structure developed for fixed base redundant manipulators. This structure relies on the *end-effector dynamic model* obtained by projecting the mechanism dynamics into the operational space, and the *dynamically consistent force/torque relationship* that provides decoupled control of joint motions in the null space associated with the redundant mechanism.

Another important issue in mobile manipulation concerns cooperative operations between multiple vehicle/arm systems [1,39]. An example of cooperative operations involving multiple vehicle/arm systems in construction tasks is illustrated in Fig. 5.

The *augmented object* and *virtual linkage* models we developed for fixed base multi-arm robots have

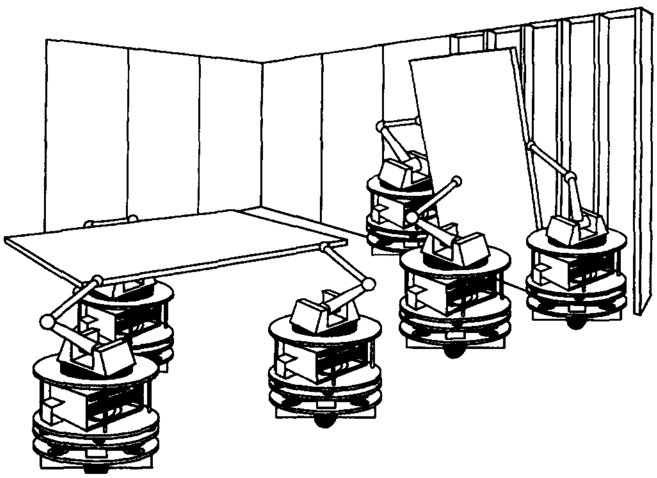

Fig. 5. Robotics in construction: Drywall.

been extended to multiple vehicle/arm systems. For fixed base manipulation, the *augmented object* and *virtual linkage* models have been implemented in an architecture that requires some level of centralized control, which is not quite suited for multiple autonomous mobile manipulation platforms.

In a multiple mobile robot system, each robot has real-time access only to its own state. Recently, we have developed [20] a decentralized control structure. In this structure, the object-level specifications of the task are transformed into individual tasks for each of the cooperative robots. Local feedback control loops are then developed at each grasp point. The task transformation and the design of the local controllers are accomplished in consistency with the *augmented object* and *virtual linkage* models.

These developments are being implemented on two autonomous mobile manipulation platforms we have designed and built at Stanford in collaboration with Nomadic Technologies and Oak Ridge National Laboratories.

Each platform consists of a PUMA 560 arm mounted on a holonomic mobile base, as shown in Fig. 6. The PUMA manipulator is equipped with a six-axis force sensor on the wrist, and an electric two-fingered gripper. The base consists of three "lateral" orthogonal universal-wheel assemblies which allow the base to translate and rotate holonomically in relatively flat office-like environments [25].

These robots have been used to demonstrate various operations involving arm/vehicle dynamic coordination, motion and force control, and cooperative manipulation [19].

3. Basic fine motion primitive

Planning fine motion tasks and controlling them are two difficult and challenging problems. A major difficulty in dealing with such tasks is associated with uncertainties. Uncertainties in sensing and control along with tolerances in mating parts, fixtures, and tools all contribute to uncertainty in the relative positions of mating parts. The accommodation of uncertainties with conventional robots requires costly engineering of the workplace and tedious programming of machines.

One of the most important attributes of any manipulation system is its ability to interact with the environment and perform fine motion tasks. Given the greater significance of uncertainties, force control and compliant motion control are key modalities in the development of fine motion manipulation capabilities. An effective approach for dealing with uncertainties is the development of fine motion primitives and sensor-based strategies, which recognize contacts when they occur, and take advantage of them to guide the moving object towards the goal. Sensory data (typically,

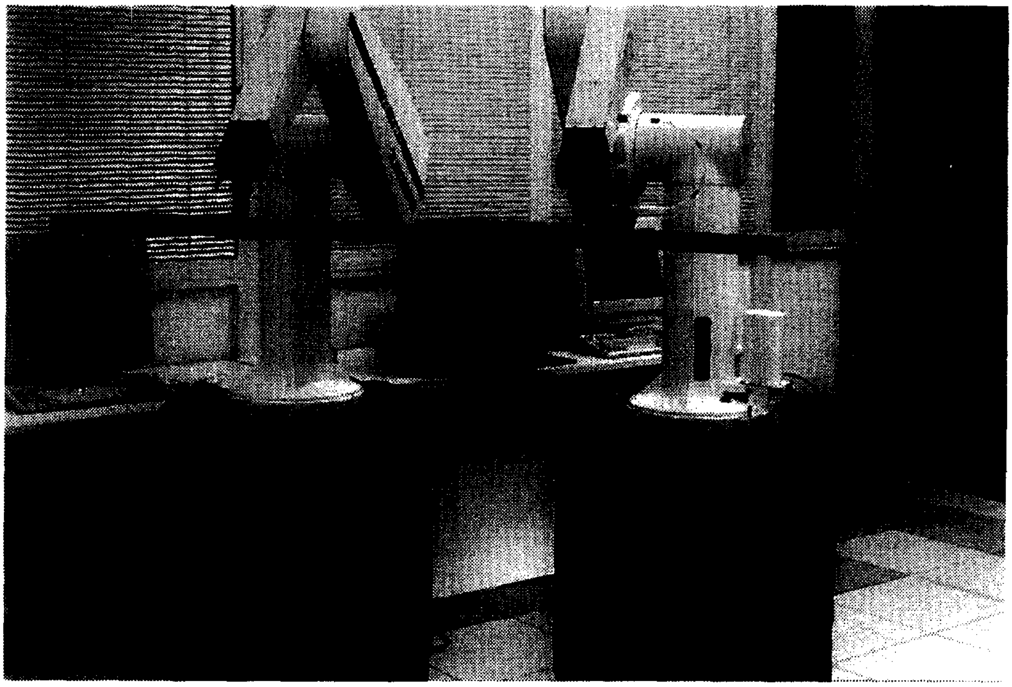

Fig. 6. Stanford mobile platforms.

force and position data) can be used during the motion to adapt the path to the actual geometry of the object, e.g., by sliding along the surface.

With the object-level manipulation capabilities it provides, the operational space formulation constitutes a natural framework for the control of fine motion operations. With this approach, the user specifies motions and compliances directly at the object level, while the coordination and control of the various manipulators involved in the task are performed by a transparent dynamic controller. Because of its multi-effector ability, an operational space controller is also capable of dealing with assemblies containing parts which span several orders of magnitude in scale.

Objects are likely to make contact at configurations in the surroundings of the planned configuration. Different contact configurations of mating parts results in different reaction forces on the manipulated object. A sensor-based strategy relies on an appropriate selection of compliant motion parameters such that, for all possible reaction forces, the resulting motion of the object is towards the goal.

The operational space framework provides a *basic primitive* for object motion and force control. This primitive is parametrized by compliance frames, the operational point, generalized selection matrices, and desired motion and forces.

$$\boldsymbol{F} = \boldsymbol{F}(\text{Operational-point, Compliant frame, Desired motions, Desired forces}).$$

By selecting these parameters appropriately, one can instantiate this basic control model in many different ways to adapt to the needs of specific tasks. Such strategies have been explored for several tasks including insertion, face-to-face object stacking, and surface following operations. The effectiveness of these strategies in executing constrained motion operations under relaxed uncertainty conditions has been demonstrated on various tasks [30].

4. Elastic band

To perform motion tasks, a robot must combine the ability of planning motions and executing them. Since a planned motion is based on as a priori knowledge of the environment, it is difficult to carry out such a motion when uncertainties and unexpected obstacles are to be considered. Reactive behaviors sought to deal with dynamic environments are, by their local nature, incapable of achieving global goals. Our investigation of a framework to connect real-time collision avoidance capabilities with a global planning system has resulted in a new approach based on the *elastic band* concept [27].

An elastic band is a deformable collision-free path. The initial shape of the elastic is the path generated by a planner. Subjected to artificial forces [13], the elastic band deforms in real time to a short and smooth path that maintains clearance from the obstacles. The elastic continues to deform as changes in the environment are detected by sensors, enabling the robot to accommodate uncertainties and react to unexpected and moving obstacles. An important characteristic of the elastic band is that it preserves the global nature of the initial trajectory since the artificial forces are applied to the robot path instead of directly to the robot.

An elastic band is a one-dimensional continuous solid described by a parametrized function $\boldsymbol{c}(s)$ of particle s, where $s \in [0, 1]$. An elastic band involves three artificial forces: an internal contraction force $f_{\text{int}}(s)$, a repulsive force $f_{\text{ext}}(s)$, and a constraint force $f_{\text{const}}(s)$. The contraction force simulates the tension in a stretched elastic band and removes any slack in the path, thus improving the shape of the initial path. The repulsive force maintains the clearance of the elastic band from obstacles. The constraint force prevents particles from moving along the elastic. The total force applied to a particle s is

$$f(s) = f_{\text{int}}(s) + f_{\text{ext}}(s) + f_{\text{const}}(s). \tag{21}$$

These forces deform the elastic until equilibrium is reached. The appearance of new obstacles or the detection of uncertainties in the environment modify the forces on the elastic, causing it to deform to a new equilibrium position, as illustrated in Fig. 7. Obviously, if the changes in the environment are large, the elastic band could fail to remain in a collision-free path even if one exists, e.g., closing the door through which a robot had planned to move. In such a situation, the failure is detected and the planner is recalled.

A major challenge in implementing the elastic band framework for robots with many degrees of freedom is achieving real-time performance. The difficulty arises because the elastic band must remain in the free space

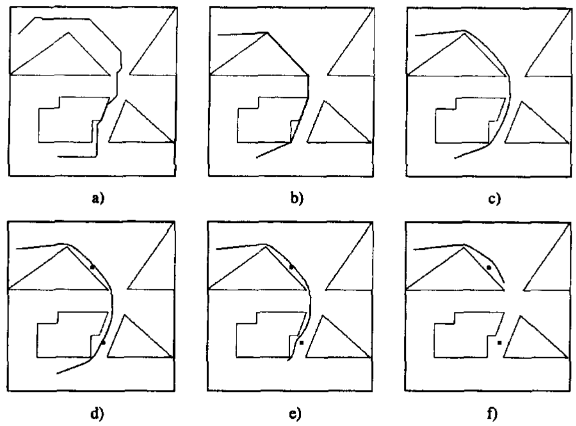

Fig. 7. The elastic band: (a) A path generated by a planner: (b) application of internal contraction forces: (c) application of both contraction and repulsion forces: (d) some unknown obstacles on the path: (e) and (f) avoidance of the unknown obstacles during execution.

of the robot. The determination of whether a path lies in the free space is difficult because the generation of the free space is computationally expensive. This difficulty has been addressed using a representation of the elastic band as a series of *bubbles* in the free space.

The key to implementing elastic bands in high dimensional configuration spaces is the *bubble* concept. A bubble is a local region of the free space around the robot configuration. Each region is computed by examining the local freedom of the robot at a given configuration.

For the two-degree-of-freedom robot shown in Fig. 8, the bubble denoted $B(\boldsymbol{x})$ at a given configuration $\boldsymbol{x}$ can be defined by the circle centered at that configuration with a radius $\underline{\rho}(\boldsymbol{x})$, that represents the shortest distance between the robot at $\boldsymbol{x}$ and the obstacles in the environment.

$$B(\boldsymbol{x}_i) = \{\boldsymbol{x}: \|\boldsymbol{x} - \boldsymbol{x}_i\| < \underline{\rho}(\boldsymbol{x})\}. \tag{22}$$

With bubbles, an elastic band is represented by a finite series of bubbles, constructed from a series of configurations or via points for the robot. To ensure that a collision-free path can be generated between the via points, we impose that bubbles at consecutive via points overlap.

This bubble representation of an elastic band has the desirable property that the complexity of the representation is related to the complexity of the situation.

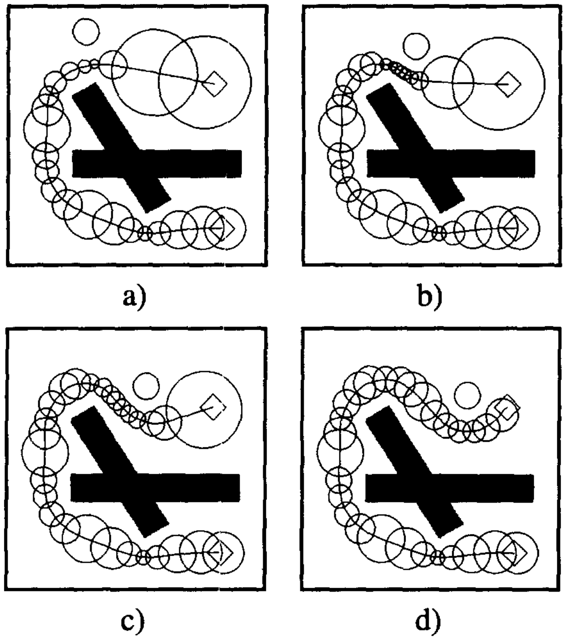

Fig. 8. Bubble implementation of elastic band. As an obstacle moves, the bubbles also move to minimize the force on the elastic band. If needed, bubbles are inserted and deleted to maintain a collision free path.

When the robot is far from obstacles, the bubbles tend to be large and can hence be spaced far apart. In contrast, if the robot is maneuvering close to an obstacle then the bubbles would be smaller and more bubbles are required to describe the elastic band.

Bubbles can be generated efficiently for robots with many degrees of freedom. Fig. 9 shows the configurations used to represent an elastic for a planar six-degree-of-freedom manipulator. The configuration space and bubbles for this example have dimension six. In this illustration, the bubbles associated with the particles of the elastic are not shown due to the difficulties in displaying six-dimensional objects. Although they are not displayed, the bubbles associated with successive particles overlap each other.

The computational effort required to generate a bubble is dominated by the necessary distance computations. We have developed a novel algorithm for efficiently computing the distance between non-convex objects [26]. The algorithm is based on a combination of a hierarchical bounding representation, a simple search routine, and a convex distance algorithm.

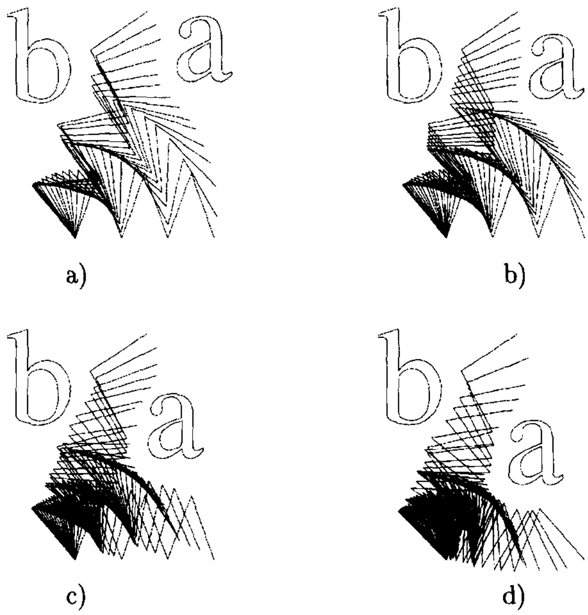

Fig. 9. An elastic band for a six-degree-of-freedom manipulator. The elastic band for a manipulator deforms to avoid obstacles.

To move a robot along a path requires a time-parametrization. We have developed an incremental time-parametrization algorithm that generates a discrete approximation to the time-optimal trajectory. The generation of the parametrization can be overlapped with the motion of the robot, effectively eliminating the time-cost of the algorithm.

This approach has been experimentally demonstrated on two PUMA 560 manipulators operating in a shared environment [26].

5. Conclusion

In this article, we have presented the various models and methodologies developed in the operational space framework for providing robot systems with object-level manipulation capabilities. These capabilities are the basis for the development of fine motion primitives and sensor-based compliant motion strategies for generic part mating operations. We have also presented the elastic band, which constitutes an effective framework to deal with real-time collision-free motion control for a robot operating in an evolving environment. Implemented as a real-time servo-loop, an elastic band provides many of the benefits of reactive systems without sacrificing global planning.

Acknowledgements

The financial support of Boeing, General Motors, Hitachi Construction Machinery, and NSF (grants IRI-9320017 and CAD-9320419) is gratefully acknowledged.

References

[1] J.A. Adams, R. Bajcsy, J. Kosecka, V. Kumar, R. Mandelbaum, M. Mintz, R. Paul, C. Wang, Y. Yamamoto and X. Yun, Cooperative material handling by human and robotic agents: Module development and system synthesis, *Proc. IEEE/RSJ Int. Conf. on Intelligent Robotics and Systems* (1985) 200–205.

[2] J.S. Albus, A theory for intelligent machine systems, *Proc. IROS'91 Int. Workshop on Intelligent Robots and Systems* (1991) 3–9.

[3] C.O. Alford and S.M. Belyeu, Coordinated control of two robot arms, *Proc. IEEE Int. Conf. on Robotics and Automation* (1984) 468–473.

[4] J. Barraquand and J.C. Latombe, Robot motion planning: A distributed representation approach, *International Journal of Robotics Research* 10 (6) (1991).

[5] K. Chang and O. Khatib, Manipulator control at kinematic singularities: A dynamically consistent strategy, *Proc. IEEE/RSJ Int. Conf. on Intelligent Robots and Systems*, Pittsburgh, Vol. 3 (1995) 84–88.

[6] R. Chatila, R. Alami, B. Degallaix and H. Laruelle, Integrated planning and execution control of autonomous robot actions, *Proc. IEEE Int. Conf. on Robotics and Automation* (1992) 2689–2696.

[7] S. Chiaverini, B. Siciliano and O. Egeland, Experimental results on controlling a 6-DOF robot manipulator in the neighborhood of kinematic singularities, *Proc. 3rd Int. Symp. on Experimental Robotics*, Kyoto, Japan (1993).

[8] H. Hanafusa, T. Yoshikawa and Y. Nakamura, Analysis and control of articulated robot arms with redundancy, *8th IFAC World Congress* XIV (1981) 38–83.

[9] S. Hayati, Hybrid position/force control of multi-arm cooperating robots, *Proc. IEEE Int. Conf. on Robotics and Automation* (1987) 1375–1380.

[10] N. Hogan, Impedance control of industrial robots, *Robotics and Computer-Integrated Manufacturing* 1 (1) (1984) 97–113.

[11] J.M. Hollerbach and K.C. Suh, Redundancy resolution of manipulators through torque optimization, *Proc. IEEE Int. Conf. on Robotics and Automanon* (1985) 1016–1021.

[12] O. Khatib, Commande Dynamique dans l'Espace Opérationnel des Robots Manipulateurs en Présence d'Obstacles, Thése de Docteur-Ingénieur, École Nationale Supérieure de l'Aéronautique et de l'Espace, Toulouse, France (1980).

[13] O. Khatib, Real-time obstacle avoidance for manipulators and mobile robots, *International Journal of Robotic Research* 5 (1) (1986) 90–98.

[14] O. Khatib, A unified approach to motion and force control of robot manipulators: The operational space formulation, *IEEE Journal on Robotics and Automation* 3 (1) (1987) 43–53.

[15] O. Khatib, Object manipulation in a multi-effector robot system, in: Robotics Research, R. Bolles and B. Roth, eds., Vol. 4 (MIT Press, Cambridge, MA, 1988) 137–144.

[16] O. Khatib, Reduced effective inertia in macro/mini-manipulator systems, in: *Robotics Research*, H. Miura and S. Arimoto, eds., Vol. 5 (MIT Press, Cambridge, MA, 1990) 279–284.

[17] O. Khatib, Inertial properties in robotics manipulation: An object-level framework, *International Journal of Robotics Research* 14 (1) (1995) 19–36.

[18] O. Khatib and J.F. Le Maitre, Dynamic control of manipulators operating in a complex environment, *Proc. 3rd CISM-IFToMM Symp. on Theory and Practice of Robots and Manipulators* (1978) 267–282.

[19] O. Khatib, K. Yokoi, K. Chang, D. Ruspini, R. Holmberg, A. Casal and A. Baader, The robotic assistant, *IEEE Int. Conf. Robotics and Automation Video Proc.* (1996).

[20] O. Khatib, K. Yokoi, K. Chang, D. Ruspini, R. Holmberg, A. Casal and A. Baader, Force strategies for cooperative tasks in multiple mobile manipulation systems, *Robotics Research,* T. Kanade and R. Paul, eds., Vol. 6, IFRR: The International Foundation for Robotics Research.

[21] V. Kumar and K.J. Waldron, Force distribution in closed kinematic chains. *Proc. IEEE Int. Conf. on Robotics and Automation*, Philadelphia, PA (1988) 114–119.

[22] J.Y.S. Luh, M.W. Walker and P. Paul, Resolved acceleration control of mechanical manipulators, *IEEE Transactions on Automatic Control* (3) (1980) 468–474.

[23] Y. Nakamura, Kinematical studies on the trajectory control of robot manipulators, Ph.D. Thesis, Kyoto, Japan (1981).

[24] Y. Nakamura, Minimizing object strain energy for coordination of multiple robotic mechanisms, *Proc. American Control Conf.* (1988) 499–504.

[25] F.G. Pin and S.M. Killough, A new family of omnidirectional and holonomic wheeled platforms for mobile robots, Oak Ridge National Laboratory Technical Reports (1994).

[26] S. Quinlan, *Real-time modification of collision-free paths*, Ph.D. Thesis, Report No. STAN-CS-TR-95-1537, Stanford University (1995).

[27] S. Quinlan and O. Khatib, Elastic bands: Connecting path planning and robot control, *Proc. IEEE Int. Conf. on Robotics and Automation*, Atlanta, GA, Vol. 2 (1993) 802–807.

[28] M. Raibert and J. Craig, Hybrid position/force control of manipulators, *ASME Journal of Dynamic Systems, Measurement, and Control* (1981) 126–133.

[29] J.K. Salisbury, Active stiffness control of a manipulator in cartesian coordinates, *Proc. 19th IEEE Conf. Decision and Control* (1981).
[30] S. Shekhar and O. Khatib, Force Strategies in real-time fine motion assembly, *Proc. ASME Winter Annual Meeting*, Boston, MA (1987) 169–176.
[31] K. Takase, Task-oriented variable control of manipulator and its software servoing system, *Proc. IFAC Int. Symp.* (1977).
[32] T.J. Tarn, A.K. Bejczy and X. Yun, Design of dynamic control of two cooperating robot arms: Closed chain formulation, *Proc. IEEE Int. Conf. on Robotics and Automation* (1987) 7–13.
[33] M. Uchiyama and P. Dauchez, A symmetric hybrid position/force control scheme for the coordination of two robots, *Proc. IEEE Int. Conf. on Robotics and Automation* (1988) 350–356.
[34] D.E. Whitney, Resolved motion rate control of manipulators and human prostheses, *IEEE Transachons on Man, Machine, and Systems* 10 (2) (1969) 47–53.
[35] D.E. Whitney, Force feedback control of manipulator fine motions, *ASME Journal Dynamic Systems, Measurement, and Control* (1977) 91–97.
[36] D. Williams and O. Khatib, The virtual linkage: A model for internal forces in multi-grasp manipulation, *Proc. IEEE Intl. Conf. on Robotics and Automation*, Atlanta, GA (1993) 1025–1030.
[37] D. Williams and O. Khatib, Multi-grasp manipulation, *IEEE Int. Conf. on Robotics and Automation Video Proc.* (1995).
[38] Y.F. Zheng and J.Y.S. Luh, Joint torques for control of two coordinated moving robots, *Proc. IEEE Int. Conf. on Robotics and Automation* (1986) 1375–1380.
[39] Y.F. Zheng and J.Y.S. Luh, Joint torques for control of two coordinated moving robots, *Proc. IEEE Int. Conf. on Robotics and Automation* (1986) 1375–1380.

Oussama Khatib received the Ph.D. degree in 1980 from Sup'Aéro Toulouse, France. He is an Associate Professor of Computer Science and (*by courtesy*) Mechanical Engineering at Stanford University. His research is in task-oriented sensor-based mobile robotic manipulation, with emphasis on the connection between robot planning and control. He is also working on the design and development of a new generation of high-performance force-controlled robot systems.

Sean Quinlan received the B.Sc. degree in computer science from Sydney University, Australia in 1988, and completed the Ph.D. degree in computer science at Stanford University in 1994. He is currently a Member of Technical Staff at Bell Labs, Lucent Technologies. His research interests include robotics, operating systems, and computer graphics.

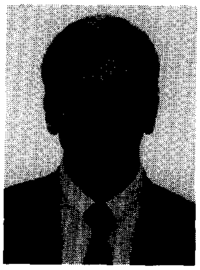

David Williams received the B.E. degree in mechanical/materials engineering from Vanderbilt University in 1987, and completed the M.S. and Ph.D. degrees in mechanical engineering at Stanford University in 1988 and 1995, respectively. He is currently a Senior Business Analyst at Capital One, where his responsibilities include strategic development and implementation of new product marketing efforts. His research interests include multi-arm coordination, force control, and real-time control of non-linear systems, as well as dynamic simulation.